Repeated load triaxial tests of wicking nonwoven geotextile and geogrid composite stabilized base materials

Jiming Liu[1], *Cheng* Lin[1*], *Minghao* Liu[1], and *Sam* Bhat[2]

[1] Department of Civil Engineering, University of Victoria, Victoria, British Columbia V8P 5C2, Canada
[2] Titan Environmental Containment LTD., Ile des Chenes, Manitoba R0A 0T1, Canada

Abstract. In road construction, geogrids are frequently used to stabilize the base course through their lateral confinement applied to the base materials. Wicking fabrics are also used to improve road performance by installing them at the road base and subgrade interface to remove water from the road and reduce the build-up of pore water pressure while providing a separate function to mitigate the weak subgrade intrusion into the base course. However, the combined use of these two materials on the road has not been reported. This study aims to investigate the effectiveness of using an innovative geosynthetic composite called WickGrid™ in stabilizing the base materials. This geosynthetic material is made by high stiffness biaxial polypropylene (PP) geogrid, heat bonded to a continuous filament nonwoven geotextile having wicking properties. To achieve the objectives, repeated load triaxial tests were conducted on sand materials to evaluate the improvement of the base materials in accordance with the AASHTO T 307-99 (2021). The specimens were stabilized with the wicking nonwoven geotextile and geogrid composite placed at the mid-height of the specimens. Meanwhile, unstabilized specimens and specimens stabilized with biaxial geogrids were also tested for comparison. The outcomes of these tests would allow for quantifying the beneficial effects of the wicking nonwoven geotextile-geogrid composite on the improvement of road bases.

1 Introduction

1.1 Geogrid stabilization

Geogrids have been extensively employed in soil stabilization, offering better performance and increased service life. Specifically in the realm of road construction, geogrids are typically placed at the interface of base course and subgrade/subbase to increase the load distribution capacity and reduce the rate of base degradation. Geogrids increase the load distribution capacity by providing lateral confinement with friction/interlocking to

* Corresponding author: chenglin918@uvic.ca

aggregates, thus increasing the modulus of base course. As a result, the amplitude of stress distributed to subbase/subgrade is reduced [1,2].

In the domain of roadways, cyclic plate load tests and repeated load triaxial (RLT) tests are often favored due to their particular utility in simulating the conditions that pavement materials undergo due to traffic loads. Brown et al. [3] employed a model test apparatus with repeated axial loads to explore the key parameters that influence geogrid stabilization in railway ballast. They found that 1) the stabilization effect was more pronounced for a soft subgrade than a stiff one; 2) The geogrid stabilization did not offer significant increase in resilient modulus of the ballast. Moghaddas-Nejad and Small [4] conducted a series of RLT tests on geogrid-stabilized aggregates and silica sands under different levels of confining and deviator stresses. Their results demonstrate that the geogrid significantly reduced the permanent strain in the specimens, while it has limited influence on the resilient modulus of the specimens. Subsequent research has corroborated these findings, confirming that while incorporation of a geogrid may not significantly increase the resilient modulus of aggregates, it can markedly reduce permanent strain during the tests [5–7].

Lateral confinement provided by geogrids can also serve to stabilize sandy soils. However, it is important to note that when the aperture-to-mean particle size ratio is particularly large, the gains in strength and stiffness may not be as pronounced as those observed in aggregates [2,8]. Geogrid-stabilized sand is more common in the context of foundation engineering, as geogrid-stabilized soils under footings are frequently seen in literature. According to both model tests and numerical studies, the incorporation of a geogrid has been shown to enhance the bearing capacity and mitigate the settlement of sand under footings [9–11].

1.2 Wicking geotextiles

Wicking geotextiles are specialized geotextiles fabricated from unique fibers capable of generating substantial capillary forces. These forces enable the material to draw water away from the surrounding soil. In roadway applications, wicking geotextiles are commonly installed in such a way that a portion of the fabric remains exposed to the atmosphere. This configuration leverages the relative humidity differences between the air and the soil within the road structure, allowing the wicking geotextiles to transfer moisture out of the road and facilitate its evaporation into the air. When positioned at the interface between the base course and the subgrade, wicking geotextiles serve the purpose of providing lateral drainage. This drainage includes water from the aggregates, which is moved by gravitational forces, as well as water from the subgrade, which is transported via capillary action.

Wang et al. [12] provided evidence that wicking geotextiles could facilitate lateral gravitational drainage when the aggregate base was in a saturated condition and continue to enable wicking drainage even when the aggregate base was not saturated. Zhang et al. [13] reported the application of wicking geotextiles to address freeze-thaw challenges in a road located in Alaska, USA. In this case, two layers of wicking geotextiles were incorporated into the road structure to counteract water accumulation in the base course, which could arise from both rainfall and capillary action. The implementation of wicking geotextiles effectively lowered the moisture content in the base course following periods of rainfall and substantially alleviated issues related to frost boils and soft spots.

It's noteworthy that the majority of studies focusing on the application of wicking geotextiles in roadways have predominantly employed woven wicking geotextiles. The literature on the use of nonwoven wicking geotextiles in geotechnical engineering is comparatively sparse. Zornberg et al. [14] conducted laboratory tests to examine the efficacy of wicking geotextiles. Their infiltration column tests revealed that nonwoven geotextiles

containing wicking fibers could effectively mitigate moisture accumulation caused by capillary barriers, provided that lateral drainage was permitted.

However, the combined use of geogrids and wicking geotextiles on the road has not been reported in existing literature. To address this gap, an innovative geosynthetics material namely WickGrid^{TM} has been introduced, amalgamating the advantages of both geogrids and wicking geotextiles. This geosynthetics material is a high stiffness biaxial polypropylene (PP) geogrid, heat-bonded to a continuous filament nonwoven geotextile having wicking properties. The present study aims to assess the efficacy of this wicking nonwoven geotextile and geogrid composite as a stabilizing agent through a series of element-scale RLT tests, offering a preliminary evaluation of its potential benefits for road applications.

2 Materials and Methods

2.1 Materials

For comparative analysis, this study incorporates an unstabilized specimen, a geogrid-stabilized specimen, and the wicking nonwoven geotextile- geogrid composite stabilized specimen in the RLT tests. The properties of the materials used in these tests are detailed below.

2.1.1 Sand

Sand employed in the RLT tests exhibited a mean particle size (D_{50}) of 0.72 mm, a coefficient of uniformity of 4.43, and a coefficient of curvature of 0.87. The gradation is depicted in Fig. 1. The sand's specific gravity is 2.71, and its maximum dry density is 1.903 g/cm³ at an optimum water content of 10.1%, as determined by the standard Proctor compaction test [ASTM D698-12(2021), Method A]. The sand was compacted to achieve this dry density and moisture content in the specimen.

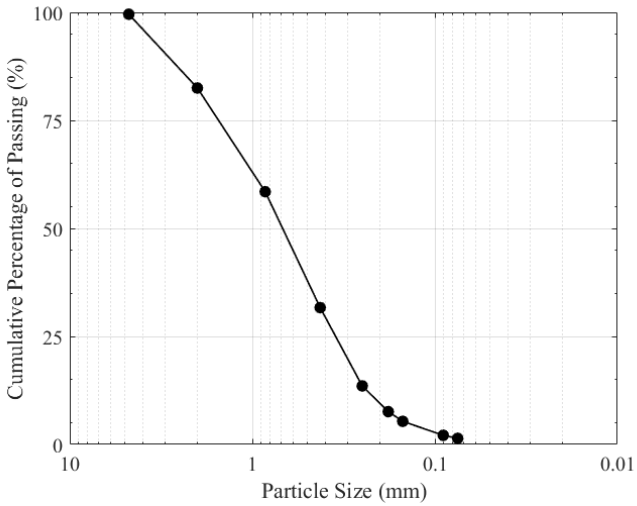

Fig. 1. Particle size distribution of the sand

2.1.2 Geosynthetics

This study utilises the wicking nonwoven geotextile-geogrid composite, a product provided by Titan Environmental Containment Ltd. This composite comprises a high-stiffness, biaxial polypropylene (PP) geogrid that is thermally bonded to a continuous filament nonwoven geotextile with wicking capabilities. For the sake of brevity, the wicking nonwoven geotextile-geogrid composite will henceforth be referred to as 'the composite' in this paper.

The geogrid employed in this study is Gladiator Grid^{TM}550, which closely resembles the geogrid used in the composite. According to the specification provided by the manufacturer, both types share identical radial stiffness at 0.5% strain. The only notable difference lies in the aperture size: The geogrid has an aperture size of 38.0 mm, which is marginally larger than the 34.0 mm aperture size of the geogrid incorporated into the composite. Fig. 2 displays photographs of the two geosynthetics used in the study.

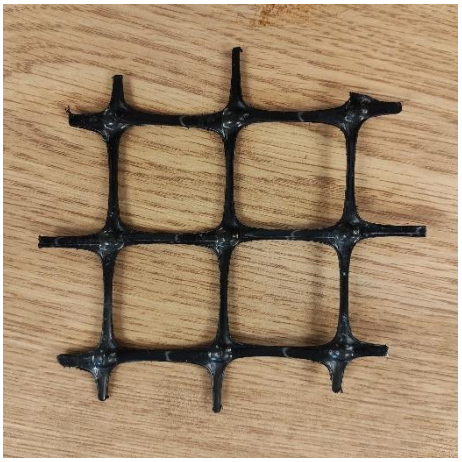

a) Geogrid

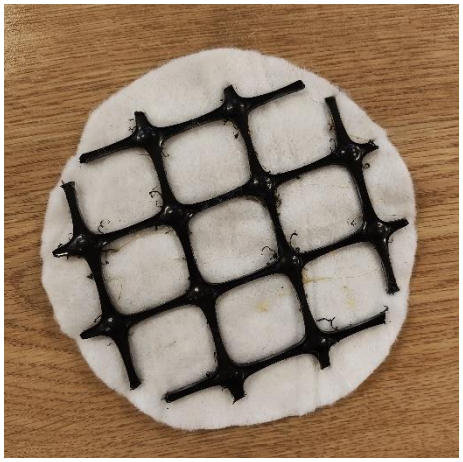

b) Wicking nonwoven geotextile-geogrid composite

Fig. 2. Photos of geogrid and the composite used in the RLT tests

2.2 Methods

2.2.1 Test procedures

The Repeated Load Triaxial (RLT) tests were conducted in accordance with the AASHTO T 307-99(2021) standard, which outlines the Method of Test for Determining the Resilient Modulus of Soils and Aggregate Materials. In alignment with this standard, cyclic loading with a frequency of 1 Hz was applied, consisting of a 0.1-second haversine load pulse followed by a 0.9-second rest period, in which only the contact stress is applied. The test specimens had dimensions of 152 mm in diameter and 305 mm in height. Testing procedures for both stabilized and unstabilized specimens adhered to the guidelines specified for base and subbase materials. Table 1 outlines the load sequence employed in the RLT tests, to which all specimens were subjected.

Table 1. AASHTO T 307 test sequence and target stress states

Sequence	Confining pressure (kPa)	Maximum Deviator Stress (kPa)	Contact Stress (kPa)	Number of cycles
Conditioning	103.4	103.4	10.3	1000
1	20.7	20.7	2.1	100
2	20.7	41.4	4.1	100
3	20.7	62.1	6.2	100
4	34.5	34.5	3.5	100
5	34.5	68.9	6.9	100
6	34.5	103.4	10.3	100
7	68.9	68.9	6.9	100
8	68.9	137.9	13.8	100
9	68.9	206.8	20.7	100
10	103.4	68.9	6.9	100
11	103.4	103.4	10.3	100
12	103.4	206.8	20.7	100
13	137.9	103.4	10.3	100
14	137.9	137.9	13.8	100
15	137.9	275.8	27.6	100

2.2.2 Specimen preparation

The sand was conditioned to its optimum moisture content prior to compaction. Specimen preparation was guided by density control, with the sand being compacted in six layers. Each layer was compacted to reach the target density corresponding to maximum dry density before proceeding to the next.

For the stabilized specimens, either the composite or geogrid was inserted at the mid-height of the specimen, following the completion of the third layer's compaction. All specimens were compacted to the same density, corresponding to the sand's maximum dry density. The mass and volume of the geosynthetics were considered negligible and were therefore disregarded.

Immediately following the RLT tests, each specimen was promptly removed from the test chamber. The specimens were then sectioned into 12 layers, each 25.4 mm thick, and the moisture content of each soil layer was subsequently determined.

3 Results and discussion

3.1 Resilient modulus

Fig. 3 plots resilient modulus against bulk stress. The geogrid-stabilized sand exhibited a higher resilient modulus than both the composite-stabilized and unstabilized sand specimens, while the composite-stabilized specimen exhibited the lowest resilient modulus among the three.

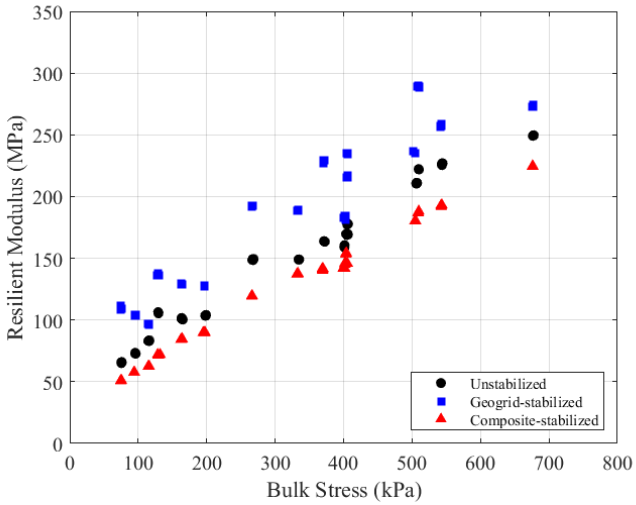

Fig. 3. Resilient modulus versus bulk stress

Previous studies suggested that the geogrid stabilization should exert limited influence on the resilient modulus in RLT tests [3–7,15]. Intriguingly, the inclusion of geotextile in the composite-stabilized specimen resulted in a resilient modulus lower than that of the unstabilized specimen. Further statistical analysis and research are required to confirm and investigate this unexpected phenomenon.

Table 2 presents the material parameters derived from the test results, with the following equation for constitutive model to predict the resilient modulus M_r:

$$M_r = k_1 P_a \left(\frac{\theta}{P_a}\right)^{k_2} \left(\frac{\tau_{oct}}{P_a} + 1\right)^{k_3}$$

In the equation, the θ is bulk stress, τ_{oct} is the octahedral shear stress, P_a is atmospheric pressure, and k_1, k_2, k_3 are the material parameters. This constitutive model is adopted by the Mechanistic-Empirical Pavement Design Guide (MEPDG).

Table 2. RM-bulk stress, with parameters using MEPDG equation

	Sand	Geogrid	The composite
k_1	749.36	1121.4	578.44
k_2	0.67652	0.68483	0.71533
k_3	-0.15091	-0.58605	-0.04249
R^2	0.97286	0.96292	0.99255

3.2 Permanent strain

The development of permanent strain with respect to load cycles is shown in Fig. 4. Both geogrid and the composite effectively mitigate the permanent strain when compared to the unstabilized sand. The disparity in permanent strain between unstabilized and stabilized sands continues to widen as loading progresses.

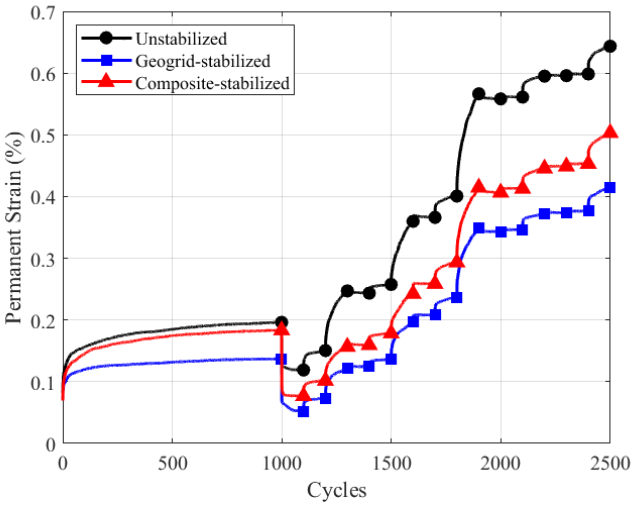

Fig.4. Accumulation of permanent strain with number of cycles

Previous experimental studies frequently utilize permanent strain as a metric to quantify the advantages of geogrid stabilization [16,15,17], highlighting its impact on the long-term performance of base materials. The superior performance of geogrid and the composite underscores their efficacy in enhancing base material behavior.

Geogrid outperformed the composite in limiting permanent deformation. A plausible explanation for this could be that the wicking nonwoven geotextile-geogrid composite creates a smaller 'stiffened zone' compared to geogrid. While geogrid enhances the mechanical properties of the soil both above and below its placement, the stiffening effect for the soil beneath the composite is partially negated by the intervening wicking geotextile. This further evidences that an open aperture geogrid performs better when placed within the granular layers due to positive mechanical interlocking of the fill particles through the geogrid apertures, whereas a geotextile-geogrid composite is expected to perform better when placed directly over the soft subgrade.

This local stiffening effect was captured by previous studies. In a study involving RLT tests on geogrid-stabilized aggregates, Byun and Tutumuler [18] observed that the shear modulus in the immediate vicinity of the geogrid was markedly higher than in areas further away, as well as in any location within an unstabilized specimen. They also established a correlation between the shear modulus and permanent strain.

3.3 Moisture content after tests

Fig. 5 provides a detailed view of the moisture content distribution by height in the specimens after the tests. The Y-axis labels correspond to the layer numbers sectioned from the top down, as described in Section 2.2.2. For example, Layers 1 and 12 represents the topmost and bottommost 25.4 mm thick layer of soil in the specimen, respectively, while the geogrid/the composite was placed between Layers 6 and 7. The wicking nonwoven geotextile-geogrid composite significantly reduced the moisture content in the soil immediately surrounding it. The layer directly beneath the composite had the lowest moisture content following the RLT tests, even surpassing the reduced moisture levels at both the top and bottom of the specimen, which are next to the drainage boundaries.

Upon the completion of the repeated loading cycles, the moisture content in nearly all layers of the specimens dropped to below 8.5%. The specimen stabilized with geogrid

retained more moisture than the other two types. Additionally, a distinct reduction in moisture content was observed at the specimen's mid-height, precisely where the geogrid was located, which might result from the localized stiffening offered by geogrid.

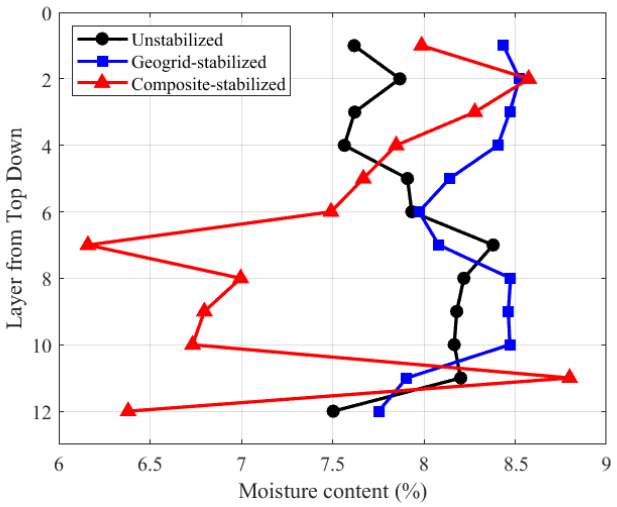

Fig.5. Moisture content across 12 layers of specimens after RLT tests

It is crucial to acknowledge the limitations of this study. Specifically, the experimental setup was at an element scale, which did not include key real-world factors such as the subgrade layer and lateral drainage. In practice, the wicking nonwoven geotextile-geogrid composite and geogrid are typically installed at the interface between the base course and subgrade, a placement that was not replicated in these RLT tests. Thus, the efficacy of the composite in lateral drainage and separation to prevent subgrade intrusion was not able to be examined in this study.

Existing research highlights the importance of exposing a portion of the wicking geotextile to the atmosphere to let the relative humidity differences drive its lateral drainage process. Although the moisture content results in this study suggest the wicking geotextile's potential to draw water from surrounding soil, the absence of lateral drainage and subgrade in the experimental design warrants further research for a more comprehensive understanding of the composite's effectiveness.

4 Conclusions

This study conducted Repeated Load Triaxial (RLT) tests on sand specimens stabilized with the wicking nonwoven geotextile-geogrid composite, as well as geogrid-stabilized and unstabilized sand specimens in comparison. The results indicate that the composite is effective in controlling permanent strain. This effectiveness can be attributed to the geogrid component of the composite, which provides stabilization to soil with lateral confinement.

The wicking geotextile component of the composite has proven to be effective in removing ambient moisture from the soil under the experimental conditions of this study. This capability could be particularly beneficial in scenarios where the soil is susceptible to water accumulation, as it could improve the overall performance and longevity of the road structure.

While the current study provides certain insights into the effectiveness of the composite, further research is warranted to validate these findings under more realistic conditions (e.g., model scale or field scale). Future studies could include model tests that consider both base

and subgrade layers and incorporate lateral drainage, thereby offering a more comprehensive evaluation of the composite's utility in practical applications.

References

1. J.P. Giroud, J. Han, Design Method for Geogrid-Reinforced Unpaved Roads. I. Development of Design Method, J. Geotech. Geoenviron. Eng. **130**, 775-786 (2004)
2. J.P. Giroud, J. Han, E. Tutumluer, M.J.D. Dobie, The use of geosynthetics in roads, Geosynthetics Int. **30**, 47-80 (2022)
3. S.F. Brown, J. Kwan, N.H. Thom, Identifying the key parameters that influence geogrid reinforcement of railway ballast, Geotext. Geomembr. **25**, 326-335 (2007)
4. F. Moghaddas-Nejad, J. Small, Resilient and Permanent Characteristics of Reinforced Granular Materials by Repeated Load Triaxial Tests, Geotech. Test. J. **26**, 152-166 (2003)
5. M. Nazzal, M. Abu-Farsakh, L. Mohammad, Laboratory Characterization of Reinforced Crushed Limestone under Monotonic and Cyclic Loading, J. Mater. Civ. Eng. **19**, 772-783 (2007)
6. B. Han, J. Ling, X. Shu, W. Song, R.L. Boudreau, W. Hu, B. Huang, Quantifying the effects of geogrid reinforcement in unbound granular base, Geotext. Geomembr. **47**, 369-376 (2019)
7. Q. Zhang, Z. Cao, Y. Cai, C. Gu, J. Wang, Experimental investigation into the cyclic behaviour of geogrid enhanced base layer aggregate through large-diameter triaxial tests, Transport. Geotech. **37**, 100851 (2022)
8. Gh. Tavakoli Mehrjardi, M. Khazaei, Scale effect on the behaviour of geogrid-reinforced soil under repeated loads, Geotext. Geomembr. **45**, 603-615 (2017)
9. A. Demir, A. Yildiz, M. Laman, M. Ornek, Experimental and numerical analyses of circular footing on geogrid-reinforced granular fill underlain by soft clay, Acta Geotech. **9**, 711-723 (2014)
10. A. Shadmand, M. Ghazavi, N. Ganjian, Load-settlement characteristics of large-scale square footing on sand reinforced with opening geocell reinforcement, Geotext. Geomembr. **46**, 319-326 (2018)
11. J-Q. Wang, L-L. Zhang, J-F. Xue, Y. Tang, Load-settlement response of shallow square footings on geogrid-reinforced sand under cyclic loading, Geotext. Geomembr. **46**, 586-596 (2018)
12. F. Wang, J. Han, X. Zhang, J. Guo, Laboratory tests to evaluate effectiveness of wicking geotextile in soil moisture reduction, Geotext. Geomembr. **45**, 8-13 (2017)
13. X. Zhang, W. Presler, L. Li, D. Jones, B. Odgers, Use of Wicking Fabric to Help Prevent Frost Boils in Alaskan Pavements, J. Mater. Civ. Eng. **26**, 728-740 (2014)
14. J.G. Zornberg, M. Azevedo, Capillary barrier dissipation by new wicking geotextile, in *Panamerican conference on unsaturated soils*, 20-22 (2013).
15. X. Yang, J. Han, Analytical Model for Resilient Modulus and Permanent Deformation of Geosynthetic-Reinforced Unbound Granular Material, J. Geotech. Geoenviron. Eng. **139**, 1443-1453 (2013)
16. M. Wayne, R.L. Boudreau, J. Kwon, Characterization of Mechanically Stabilized Layer by Resilient Modulus and Permanent Deformation Testing, Transport. Res. Record **2204**, 76-82 (2011)

17. H. Wang, M. Kang, I.I.A. Qamhia, E. Tutumluer, M.H. Wayne, H. Shoup, Evaluation of Open-Graded Aggregates Stabilized with a Multi-Axial Geogrid Using a Large-Scale Triaxial Test Set-Up, Transport. Res. Record, **2677**, 339-350 (2023)
18. Y-H. Byun, E. Tutumluer, Local stiffness characteristic of geogrid-stabilized aggregate in relation to accumulated permanent deformation behavior, Geotext. Geomembr. **47**, 402-7 (2019)